Journal of Applied Mechanics and Technical Physics, Vol. 43, No. 6, pp. 888–894, 2002

SOME FEATURES OF A TURBULENT SEPARATED FLOW AND HEAT TRANSFER BEHIND A STEP AND A RIB. 1. FLOW STRUCTURE

V. I. Terekhov, N. I. Yarygina, and R. F. Zhdanov

UDC 536.24

The influence of the shape and size of the obstacle on separated flow and heat transfer is studied experimentally. Results of investigation and comparative analysis of the hydrodynamic structure of a separated flow behind a step and a rib are presented. A principally different character of transfer processes in the separated flow behind obstacles of these types is demonstrated. The flow structure in the secondary vortex region is considered.

Introduction. The problem of intensification of heat-transfer processes has become particularly important recently for the reason of solving problems of energy savings in heat-exchange devices. One of the aspects of this problem is the passive intensification of convective heat transfer of the surface due to flow separation. For instance, in many engineering devices, such as heat-engineering equipment, combustion chambers, gas turbines, etc., heat-transfer intensification is reached by surface ribbing. Heat transfer in separated flows has not been adequately considered yet. The relationship between vortex formation and heat release has been poorly studied. Investigation of the flow structure in the vicinity of isolated obstacles allows one to find the reasons for separated flow reconstruction and the associated changes in local heat transfer. The mechanisms of the influence of flow prehistory and geometric parameters on the thermal characteristics are insufficiently examined.

The flow around a backward-facing step is the classical geometry of a separated flow, which was considered in many papers (see, e.g., [1–9]). Therefore, the results of these papers may be compared with separation caused by different isolated obstacles. At the same time, the known papers on separated flows with a transverse plate (rib) used as an obstacle (see, e.g., [10–12]) are not numerous and do not contain a comparison with separation behind a step under identical conditions. Most papers cited above deal mainly with some properties and parameters of separation in the case of a constant or weakly changing relative height of the obstacle. In the present work, we use the complex approach [13, 14] to studying the separated flow characteristics with a varied shape and height of the obstacle.

Test Conditions. The experiments were performed in a wind tunnel that is an open-ended air contour with a fan mounted at the entrance and with a 200×200 mm square test channel 600 mm long. The flow velocity above the obstacle was 20 m/sec, which corresponds to the Reynolds number based on the channel height $\mathrm{Re}_S \approx 3 \cdot 10^5$. The level of turbulence in the central region of the channel reached 1.2%. The dynamic characteristics were measured for the step (obstacle) height $H = 10$ and 20 mm.

Models 200 mm thick were used in the experiments (Fig. 1). A model with the upper part made of plexiglass was used for oil-film visualization of the separated flow on the surface behind the obstacles. The visualization composition was a mixture of offset paint and kerosene. To study dynamic losses behind the rib and step, we used a textolite matrix with 44 static pressure taps ∼0.3 mm in diameter located on the plate surface along its centerline. The back flow velocity was measured by a miniature Pitot–Prandtl tube with a 0.4-mm outer diameter.

Under identical external conditions, the flow structure in the flow core above the rib and step of the same height is approximately identical, which allowed us to perform a reliable comparative analysis of characteristics of

Kutateladze Institute of Thermal Physics, Siberian Division, Russian Academy of Sciences, Novosibirsk 630090. Translated from Prikladnaya Mekhanika i Tekhnicheskaya Fizika, Vol. 43, No. 6, pp. 126–133, November–December, 2002. Original article submitted April 8, 2002; revision submitted April 29, 2002.

 0021-8944/02/4306-0888 $27.00

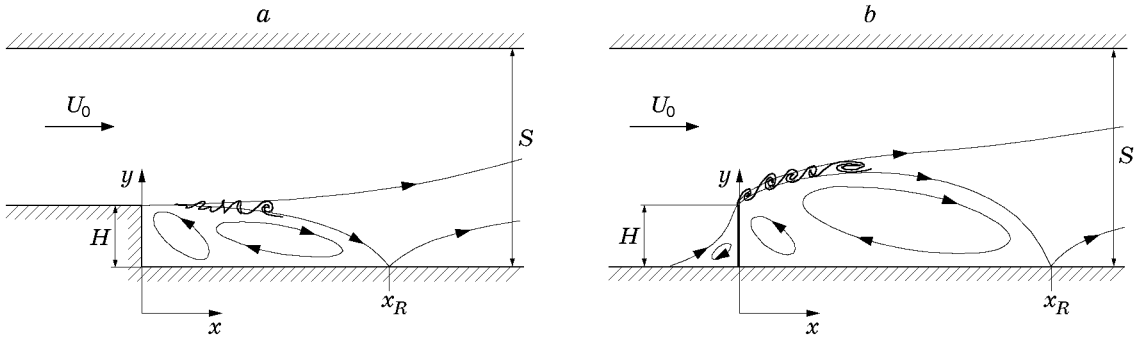

Fig. 1. Flow pattern behind a backward-facing step (a) and a rib (b).

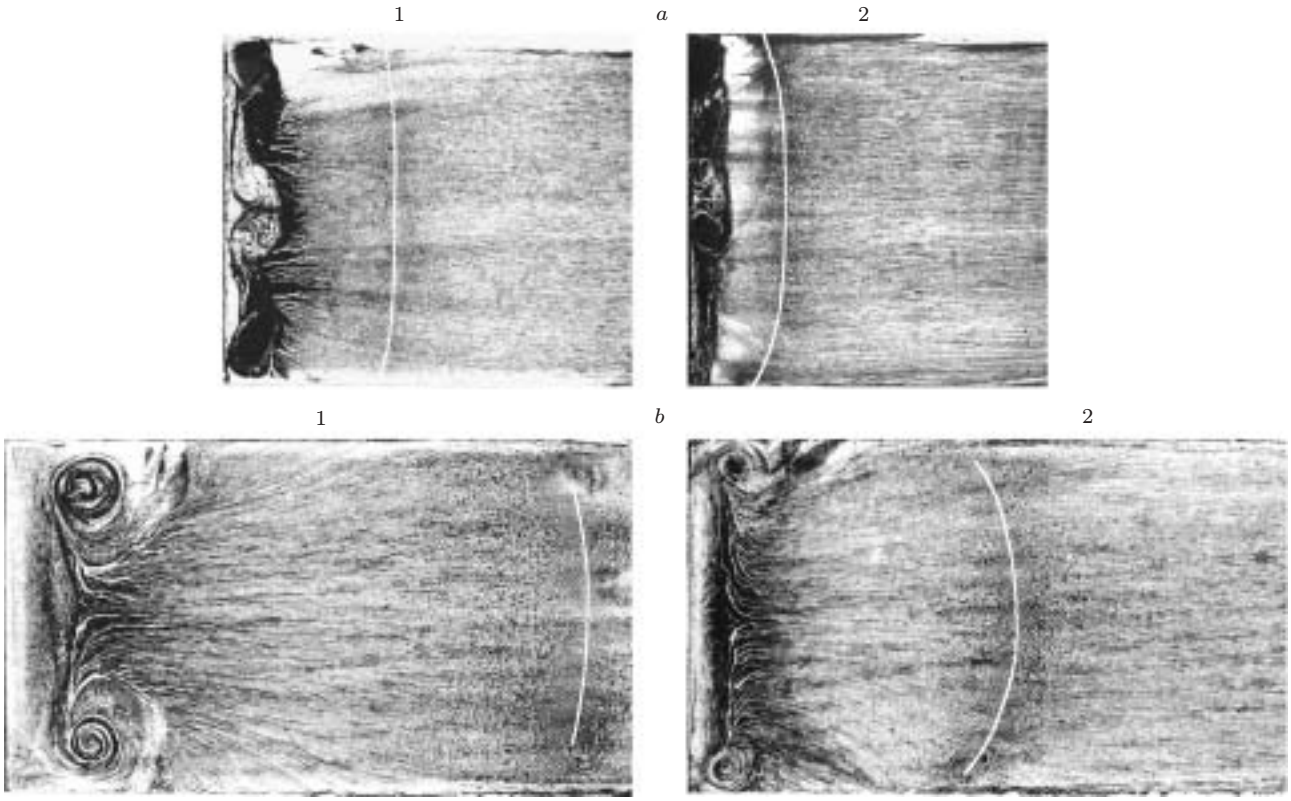

Fig. 2. Flow pattern in the separation region behind a step (a) and a rib (b) for $H = 20$ (frame 1) and 10 mm (frame 2); the white line indicates the averaged region of flow reattachment x_R.

the separated flow behind these obstacles and to reveal the degree of influence of the recirculation flow upstream of the rib on flow separation behind the latter.

Results and Discussion. Figure 2a and b shows the results of oil-film visualization of the surface behind a step and a rib, respectively (all photographs are made in the same scale; the flow direction is from left to right). It follows from Fig. 2 that the conditions of reattachment of the separated flow and formation of the secondary zone with large-scale vortices behind the step and the rib are different. Smaller vortex structures are generated in the case of separation behind the step than behind the rib and form a mixing layer [15]. These vortices collide with the surface, which leads to emergence of a reattachment region whose averaged boundary "sticks" to the side walls. This effect is not observed behind the rib, which evidences the large scale of vortices in the mixing layer. The averaged line of flow reattachment behind a step 20 mm high (frame 1 in Fig. 2a) is located at a distance $x_R/H \approx 4.8$ along the model centerline. Approaching the side walls of the channel, the averaged line of the reattachment region deforms, reaching the distance approximately equal to $4.5H$ from the step. The reattachment region is unstable; therefore, its width is approximately one half of the step height in the upstream and downstream directions. The

structure of the reattached flow in the direction of the secondary vortex deforms prior to its separation from the surface. The place of secondary separation is located at a distance of approximately $2H$ from the step along the model centerline. Thus, the transverse size of the secondary vortex varies from 20% (near the walls) to 40% of the separation bubble. A mushroom-shaped structure is noted in the central part of the secondary vortex zone. As the step height decreases by a factor of 2, the absolute size of the recirculation region decreases, and the relative length of the reattachment region is $x_R/H \approx 5.5$ ($x_R/H = 4.0$–4.5 near the side walls) (frame 2 in Fig. 2a), i.e., the curvature of the reattachment line increases significantly. This occurs because of the changed step height. The smaller the obstacle height, the smaller the radius of curvature of the reattachment line. Behind a step 10 mm high, the reattached flow, moving upstream, separates from the surface at a distance $x/H = 1.5$–2.5, and the region occupied by the secondary vortex is less than a half of the separation-region length. The structure is asymmetric and can be represented by five vortices with different shapes, sizes, and rotation intensities. The number of vortex structures in the secondary region depends on the ratio of the step height to the channel height ahead of separation and also on the channel width.

Behind a 20-mm rib (frame 1 in Fig. 2b), the averaged reattachment region along the plate centerline is localized at a distance $x_R/H \approx 16.5$, i.e., significantly further than behind a step of the same height, which is in line with results of other papers. The reattachment region behind the rib has a greater curvature than behind the step, since the influence of large spatial vortices becomes weaker with distance from the obstacle. Approaching the side walls of the channel, the reattachment line curves toward the rib, being located at a distance $x/H \approx 15.7$, which is in good agreement with the results of flow visualization behind a rib 22 mm high, which were published in [11], where $x_R/H \approx 17.2$ along the centerline and $x_R/H \approx 15$ near the side walls. After reattachment, part of the flow moves toward the obstacle (frame 1 in Fig. 2b). The flow separates from the plate surface at a distance approximately equal to $2H$ from the rib along the centerline. The length of the main recirculation vortex is greater than in the flow around the step. Powerful vortices whose size is comparable to the obstacle height are observed in the corner region, whereas they are weakly expressed in the flow behind the step. Behind a 10 mm rib, the distance to the averaged reattachment region increases up to $x_R/H \approx 18.5$ along the centerline (frame 2 in Fig. 2b) and reaches approximately $16H$ near the side walls ($z/H \approx 1.5$). The line of the reattachment region is strongly curved. As for the 20-mm rib, the length of the secondary zone in the center is approximately $2H$.

The significant difference between the flow behind a step and a rib is determined by flow prehistory. A recirculation flow is formed upstream of the rib, which affects the evolution of the mixing layer and, as will be shown below, the distribution of the pressure coefficient and the maximum velocity of the back flow. The flow structure in the secondary separation region behind 20-mm and 10-mm ribs is qualitatively identical, but it is different behind steps of the same height. This is explained by the fact that this separated flow depends on such parameters as the ratio of the channel width to the step height, the relative expansion of the channel ($ER = S/S_0$ is the ratio of the channel heights after and before expansion), and the ratio of the obstacle height to the boundary-layer thickness H/δ.

One of the main parameters that characterize the separated flow structure is the size of the reattachment region. Figure 3 shows the coordinate of the reattachment point versus the flow velocity (Reynolds number). The scatter of experimental data obtained in various works is rather large: $4.5 < x_R/H < 8.5$. Nevertheless, there is practically no influence of the Reynolds number on the recirculation-region length, if the Reynolds number varies due to changes in velocity only. At the same time, a significant effect is exerted on the reattachment-region size by the parameters H/δ (in the present work) and the degree of channel blockage (for $ER = 1.14$ and 1.25 [18]).

The static pressure distributions behind the obstacles (Fig. 4) allow one to analyze the near-wall region, which exerts a significant effect on friction, heat transfer, and separated flow structure as a whole. Figure 4 shows the pressure distributions behind a step and a rib. The pressure coefficient is determined by the formula $C_p = 2(p - p_0)/(\rho U_0^2)$, where p is the static pressure on the wall, and p_0 and U_0 are the pressure and velocity in the external flow above the step. It follows from Fig. 4a that the pressure distribution is considerably affected by the step height. First, the static pressure on the surface behind the step weakly decreases in the secondary flow region and then rapidly increases in the direction of flow reattachment. The pressure coefficient has a maximum value at a distance almost twice as large as the separation-region size (approximately by a factor of 1.5 in [6, 9]). The absolute value of the pressure coefficient increases with increasing obstacle height. In addition, an increase in the step height shifts the maximum pressure coefficient upstream. With increasing height from 10 to 20 mm, this shift is approximately $2H$. It should be noted that a similar shift of the maximum of the dependence $C_p(x/H)$ was observed in other papers (Fig. 4a).

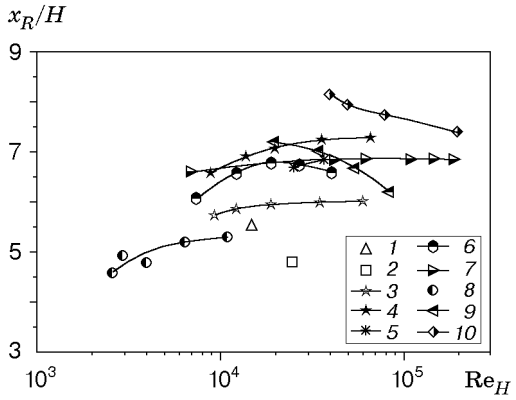

Fig. 3. Reattachment-region length as a function of the Reynolds number based on the step height for $H = 10$ mm and $ER = 1.07$ (point 1) and $H = 20$ mm and 1.14 (point 2), 1.14 [18] (points 3), 1.25 [18] (points 4), 1.2 [20] (points 5), 1.25 [3] (points 6), 1.262 [19] (points 7), 1.31 [17] (points 8), 1.64 [5] (points 9), and 1.67 [16] (points 10).

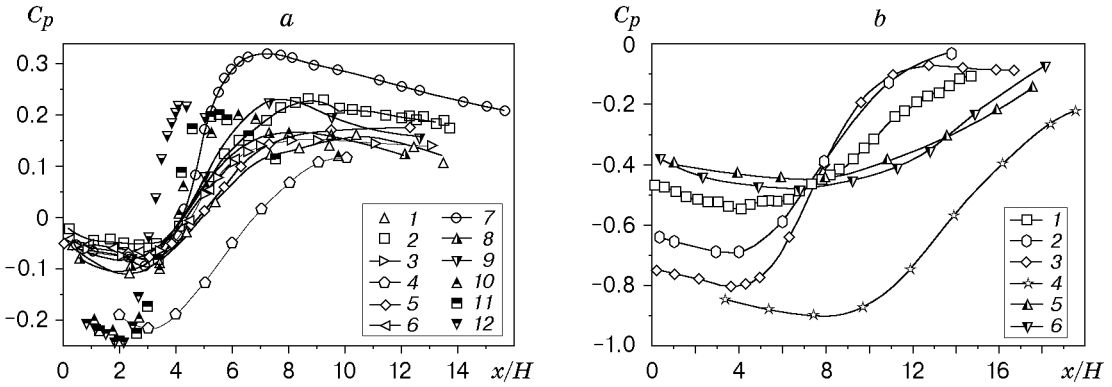

Fig. 4. Distribution of the pressure coefficient behind a step (a) and a rib (b): (a) $H = 10$ (points 1), 20 (points 2), 12.7 [6] (points 3), 15 [9] (points 4), 38 [20] (points 5), 38.1 [2] (points 6), 51 [8] (points 7), 10 [21] (points 8), 20 [21] (points 9), 12 [22] (points 10), 25 [22] (points 11), and 50 mm [22] (points 12); (b): $H = 20$ (points 1), 5 [23] (points 2), 19.05 [12] (points 3), 23.9 [10] (points 4), 15 [24] (points 5), and 30 mm [24] (points 6).

The distributions of the pressure coefficient behind the rib and the step are significantly different. Rarefaction is observed in the entire flow region behind the rib, and only approaching the reattachment point does the pressure difference tend to zero. A significant difference is also observed in the magnitude of the maximum rarefaction. We have $|C_p|_{\min} < 0.25$ behind the step, whereas rarefaction is considerably greater in the flow around the rib: $|C_p|_{\min} \to 1$ (Fig. 4b). The decrease in C_p at the initial section of the channel before reaching the minimum, as in the flow around the step, is caused by the existence of the secondary vortex.

The results obtained in different works cannot be generalized by traditional methods of processing experimental data. Interesting features of pressure behavior behind obstacles are revealed when the experimental data are presented in the form of the reduced pressure coefficient as a function of the relative streamwise coordinate (Fig. 5). The reduced pressure coefficient was determined, in accordance with [25], by the formula $\bar{C}_p = (C_p - C_{p,\min})/(1 - C_{p,\min})$, where $C_{p,\min}$ is the pressure coefficient at the point with the greatest rarefaction. It follows from Fig. 5 that the step height, in contrast to the rib height, exerts a significant effect on the dependence $C_p(x/x_R)$. This is related to additional flow separation ahead of the rib, which damps the influence of flow prehistory. The recirculation flow formed ahead of the obstacle decreases the influence of external factors: flow contraction, velocity, etc. The data on pressure coefficients behind the step cannot be generalized, since the separation is strongly affected by the relative boundary-layer thickness.

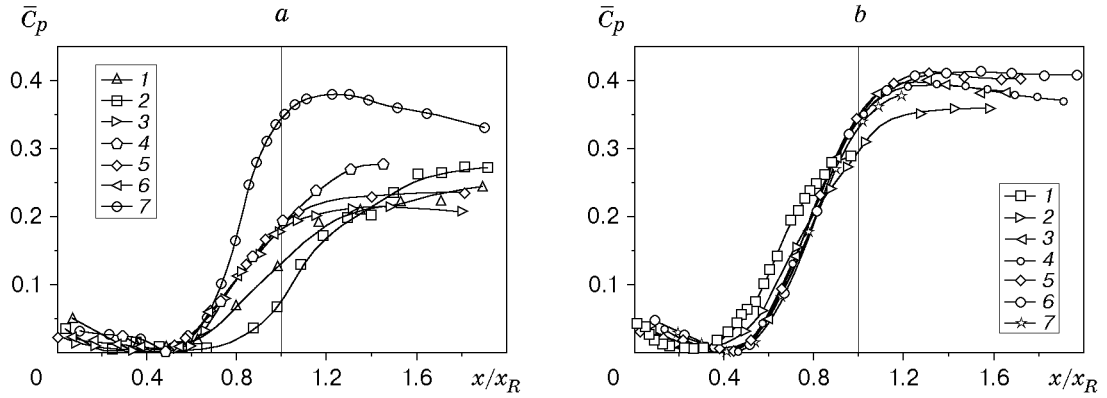

Fig. 5. Reduced pressure coefficient behind a step (a) and a rib (b): (a) $H = 10$ (points 1), 20 (points 2), 12.7 [6] (points 3), 15 [9] (points 4), 38 [20] (points 5), 38.1 [2] (points 6), and 51 mm [8] (points 7); (b) $H = 20$ (points 1), 2.4 [25] (points 2), 9 [26] (points 3), 11 [11] (points 4), 19.05 [12] (points 5), 22 [11] (points 6), and 23.9 [10] (points 7).

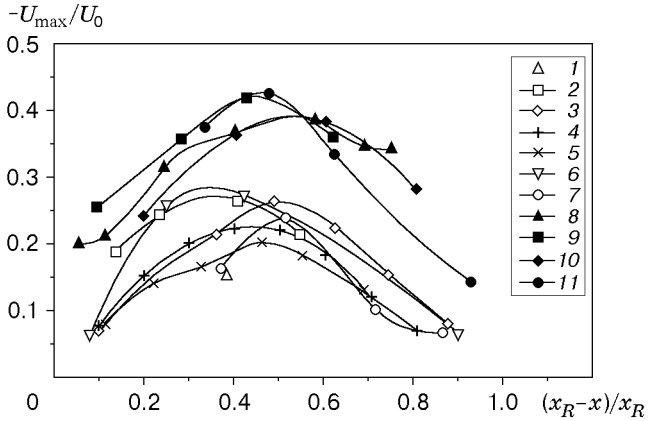

Fig. 6. Back flow velocity in the recirculation region behind a step (points 1–7) and behind a rib (points 8–11): $H = 10$ (points 1), 20 (points 2), 12 [27] (points 3), 15 [9] (points 4), 38.1 [3] (points 5), 51 [8] (points 6), 56 [28] (points 7), 10 (points 8), 20 (points 9), 10 [29] (points 10), and 22 mm [11] (points 11).

The difference in pressure distributions behind the step and the rib affects the intensity of recirculation motion in the separation region and, hence, the maximum velocity of the back flow. We obtained $-U_{\max}/U_0 < 0.3$ in experiments with the step and $-U_{\max}/U_0 > 0.4$ in experiments with the rib (Fig. 6). Thus, the recirculation flow behind the rib is more intense than that behind the step, and the absolute maximum of the back flow velocity in relative coordinates is located further from the flow-reattachment region. Since the mixing layer behind the rib is thicker and coherent structures are larger, an intense income of mass to the recirculation region occurs. With increasing obstacle height, the back flow velocity increases insignificantly.

Conclusions. It is established that the recirculation-region length, the mixing-layer thickness, and the positions of the maxima of the pressure coefficient and back flow velocity depend on the prehistory of the separated flow.

Flow visualization around a step and a rib of the same height reveal a principal difference in the separated flow structure, especially in the secondary vortex region. Thus, along with corner vortices near the side walls, additional vortices are observed in the central part near the step. Behind the rib, only large-scale corner vortex structure are observed. The reattachment region is more curved behind the rib than behind the step.

The reduced pressure coefficient behind the rib can be represented as a generalized dependence, whereas the experimental data cannot be satisfactorily generalized for the flow behind the step.

The maximum velocity of the back flow toward the step in the recirculation region is less than 30% of the free-stream velocity and exceeds 40% in experiments with the rib. With increasing obstacle height, the recirculation-flow velocity increases insignificantly.

This work was supported by the Russian Foundation for Fundamental Research (Grant No. 01-02-16842a).

REFERENCES

1. V. E. Alemasov, G. A. Glebov, and A. P. Kozlov, *Hot-Wire Methods of Investigating Separated Flows* [in Russian], Kazan' Department of the Academy of Sciences of the USSR, Kazan' (1989).
2. A. W. Adams and J. P. Johnston, "Effects of the separating shear layer on the reattachment flow structure. Part 1. Pressure and turbulence quantities," *Exp. Fluids*, **6**, No. 6, 400–408 (1988).
3. E. W. Adams and J. P. Johnston, "Effects of the separating shear layer on the reattachment flow structure. Part 2. Reattachment length and wall shear stress, *Exp. Fluids*, **6**, No. 7, 493–499 (1988).
4. J. C. Vogel and J. K. Eaton, "Combined heat transfer and fluid dynamic characteristics downstream of a backward-facing step," *Trans ASME, J. Heat Transfer*, **107**, No. 4, 922–929 (1985).
5. R. V. Westphal, J. K. Eaton, and J. P. Johnston, "A new probe for measurement of velocity and wall shear stress unsteady, reversing flow," *Trans. ASME, J. Fluids Eng.*, **103**, 478–482 (1981).
6. D. M. Driver, H. L. Seegmiller, and J. Marvin, "Time-dependent behavior of a reattaching shear layer," *AIAA J.*, **25**, No. 7, 914–919 (1987).
7. D. E. Ebbott and S. J. Kline, "Experimental investigation of subsonic turbulent flow over single and double backward-facing steps," *Trans. ASME, J. Basic Eng., Ser. D*, **84**, 317–325 (1962).
8. C. Chandrsuda and P. Bradshaw, "Turbulence structure of a reattaching mixing layer," *J. Fluid Mech.*, **110**, 171–194 (1981).
9. J. T. Yang, B. B. Tsai, and G. L. Tsai, "Separated-reattaching flow over a backstep with uniform normal mass bleed," *Trans. ASME, J. Fluids Eng.*, **116**, 29–35 (1994).
10. I. P. Castro and A. Haque, "The structure of a turbulent shear layer bounding a separation region," *J. Fluid Mech.*, **179**, 439–468 (1987).
11. R. Ruderich and H. H. Fernholz, "An experimental investigation of a turbulent shear flow with separation, reverse flow, and reattachment," *J. Fluid Mech.*, **163**, 283–322 (1986).
12. N. J. Cherry, R. Hillier, and M. E. M. Latour, "Unsteady measurements in a separated and reattaching flow," *J. Fluid Mech.*, **144**, 13–46 (1984).
13. V. I. Terekhov, N. I. Yarygina, and R. F. Zhdanov, "Effect of free-stream turbulence on heat transfer behind a rib and inclined downward step," in: *Proc. of the 11th Int. Heat Trans. Conf.* (Kyongju, Korea, August 23–28, 1998), Vol. 3, Korean Soc. of Mech. Eng., Kyongju (1998), pp. 189–194.
14. V. I. Terekhov, N. I. Yarygina, and R. F. Zhdanov, "The structure of the separated flow behind obstacles at high external turbulence," in: *Proc. of the 9th Int. Conf. on the Nethods of Aerophys. Res.* (Novosibirsk, 29 June–3 July, 1998), Part 1, Inst. of Theor. and Appl. Mech., Novosibirsk (1998), pp. 220–227.
15. R. L. Simpson, "Turbulent boundary-layer separation," *Annu. Rev. Fluid Mech.*, **21**, 205–234 (1989).
16. J. K. Eaton and J. P. Johnston, "A review of research on subsonic turbulent flow reattachment," *AIAA. J.*, **19**, 1093–1105 (1981).
17. P. L. Komarov and A. F. Polyakov, "Turbulence and heat-transfer characteristics behind a backward-facing step in a slotted channel," Preprint No. 2-396, Inst. of High Temp., Russ. Acad. of Sci., Moscow (1996).
18. A. Pyadishyus and A. Shlanchyauskas, *Turbulent Heat Transfer in Near-Wall Layers* [in Russian], Mosklas, Vil'nyus (1987).
19. Z. Jaňour and P. Jonáš, "On the flow in a channel with a backward-facing step on one wall," *Eng. Mech.*, **1**, Nos. 5/6, 313–320 (1994).
20. S. Jovic, "An experimental study of a separated/reattached flow behind a backward-facing step. $\mathrm{Re}_H = 37{,}000$," Tech. Memorandum NASA No. 110384, California (1996).
21. I. Tani, M. Iuchi, and H. Komoda, "Experimental investigation of flow separation associated with a step or groove," Report No. 364, Aeronaut. Res. Inst., Univ. of Tokyo, Tokyo (1961).
22. V. N. Kryukov, "Investigation of turbulent separation behind a streamwise located step," in: *Some Problems of Heat and Mass Exchange between Flows and Surfaces* [in Russian] (collected scientific papers), Moscow State Aviation Institute (1986), pp. 24–28.
23. Y. Nakamura and S. Ozono, "The effects of turbulence on a separated and reattaching flow," *J. Fluid Mech.*, **178**, 477–490 (1987).

24. E. V. Vlasov, A. S. Ginevskii, R. K. Karavosov, and M. O. Frankfurt, "Near-wall pressure fluctuations in the separation region behind two-dimensional obstacles," *Tr. TsAGI*, No. 2137, 3–29 (1982).
25. A. Roshko and J. C. Lau, "Some observations on transition and reattachment of free shear layer in incompressible flow," in: A. F. Charwat (ed.), *Proc. Heat Transfer and Fluid Mechanics Inst.*, Stanford Univ. Press, Stanford (1965), pp. 157–167.
26. R. Hillier and N. J. Cherry, "The effects of free-stream turbulence on separation bubbles," *J. Wind Eng. Industr. Aero.*, **8**, 49–58 (1981).
27. B. Ruck and B. Makiola, "Flow over single-sided backward-facing steps with angle variations," in: *Proc. 3rd Int. Conference on Laser Anemometry Advances and Applications*, S. N., Swansea (1989), pp. 40.1–40.10.
28. T. R. Troutt, B. Scheelke, and T. R. Norman, "Organised structures in a reattaching separated flow field," *J. Fluid Mech.*, **143**, 413–427 (1984).
29. M. Kiya and K. Sasaki, "Structure of a turbulent separation bubble," *J. Fluid Mech.*, **137**, 83–113 (1983).